Original Article

An Insight Into The Exploration At The Molecular Level About The Role Of Stringent Response In Mycobacterium Tuberculosis Dormancy

Babasaheb Shivanath Ghodke[1*], Sakshi Yadav[2]

[1*]Department of Microbiology, Dr. A.P.J. Abdul Kalam University, Indore, Madhya Pradesh, India.
[2]Department of Microbiology, Dr. A.P.J. Abdul Kalam University, Indore, Madhya Pradesh, India.

***Corresponding Author: -** Babasaheb Shivanath Ghodke

***Department of Microbiology, Dr. A.P.J. Abdul Kalam University,Indore, Madhya Pradesh, India.
E-mail: bghodke1984@gmail.com
DOI: 10.47750/pnr.2022.13.S01.291

Abstract

The infection caused by the bacteria Mycobacterium TB continues to be a major contributor to death rates around the globe. Antibiotic resistance is on the rise, and drug-resistant bacteria pose a serious danger to human health; thus, studying the causes of antibiotic tolerance is important. The lack of verified targets that allow for the elimination of chronic infections is a key barrier to the creation of new anti-tuberculosis medications. The physiological state that is regarded to be a key contributor to latent TB infection and the prolonged duration of tuberculosis therapy is one that is induced by the stringent response, which decreases replication and reduces the metabolic state under stressful situations. RelMtb is an enzyme that controls the buildup of (p)ppGpp, an effector molecule in the stringent response. Potentially useful insights into antibiotic tolerance and immune evasion, as well as novel approaches to treating TB, may result from learning to regulate this enzyme, which is thought to enable manipulation of the M. tuberculosis stringent response. The goal of this research is to get a better understanding of this route and to determine whether or not (p)ppGpp buildup is necessary to trigger the severe response. Using a combination of molecular cloning and genetic engineering, we have created a RelMtb over expression strain that is conditional but lacks the capacity to hydrolyze (p)ppGpp. Gene expression of interest is induced in this strain using an anhydrotetracycline inducing agent. Although genetic and protein evidence for inducible expression has been shown, further information is required to describe this strain and identify its true effects on (p)ppGpp and the stringent response. These results show that the aspartate route in Mtb is regulated by many metabolic pathways, plays an important role in Mtb persistence, and is a potential therapeutic target for TB treatment.

Keywords: Mycobacterium Tuberculosis, Antibiotic tolerance, Gene expression, Molecular cloning, Genetic engineering.

INTRODUCTION

The global prevalence of tuberculosis (TB) is on the rise at a rate of around 0.4% per year and is the second greatest infectious disease killer and disabler. Two million individuals lose their lives every year as a result of tuberculosis infections, which infect eight million people annually (WHO report). Small particles of Mycobacterium tuberculosis in the form of aerosol droplets are the primary cause of the disease, which manifests as a pulmonary sickness after being breathed in and deposited on the alveolar surfaces of the lungs. The development and eventual resolution of the illness may be broken down into four stages. After inhaling M. tuberculosis, the timeline of events is shown in Figure 1.

Infectious pulmonary illness caused by the bacteria Mycobacterium tuberculosis (Mtb). The disease is conveyed via the air and is carried by the droplets spat by those with an active respiratory infection. In healthy people, the immune system may be able to "wall off" the bacteria, making it difficult to identify an infection with Mtb. Active tuberculosis of the lungs is characterised by coughing up sputum or blood, chest discomfort, weakness, weight loss, fever, and night sweats. Tuberculosis treatment typically takes six months.

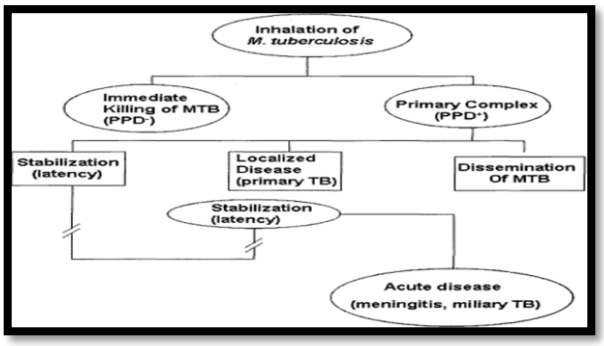

Figure 1: Chronological events after inhalation of M. tuberculosis

1. Models of persistent TB infection

As the mechanisms driving M. tuberculosis persistence and reactivation may take years to show in human hosts, several in vitro and in vivo systems have been designed to reproduce different aspects of a persistent infection. The challenges of studying infections with human hosts have led to the development of laboratory and animal models. There are limitations to each method, and none of them can perfectly simulate a human infection. These models not only provide a helpful foundation for future investigation into dormancy and its reactivation, but they also allow for such study to be conducted in greater depth.

1.1. *In vitro* Models

Wayne Model of Hypoxia-Induced Non-Replicating Persistent State

During latency, Mycobacterium TB is thought to exist in a hypoxic or anaerobic condition due to its confinement in a granuloma inside the host body, as proposed by Wayne's NRP model. By growing bacteria in an oxygen-free environment for a certain amount of time in a sealed tube, one may study the effects of hypoxia (Figure 2). Oxygen deprivation promotes a condition of non-replicating persistence similar to that of tubercle bacilli in granulomatous lesions.

The switch to NRP in bacteria has been studied under three different circumstances, all of which include the medium containing an acceptable amount of dissolved oxygen and the bacterium displaying a logarithmic growth pattern. Before the development of cell-mediated immunity in humans, M. tuberculosis was in this state. As a result of M. tuberculosis's presence in NRP-1, DNA and RNA synthesis have slowed, protein synthesis has ceased, and the dissolved O_2 level has dropped to. Many anti-mycobacterial drugs, including isoniazid and rifampicin, have been ineffective because bacteria have developed resistance to them.

Numerous gene products are also induced in bacteria, making it easier to –

1. renewable and non-renewable resources.
2. stabilise and safeguard the cell's most important components.
3. control the expression of genes involved in downstream effector pathways.

While there may be just a few bacteria in the system, the turbidity of the media increases. Once acquired immunity has developed in vivo, there is no longer any clinical difference between this and the previous state. The second to final stage, NRP-2, is characterised by a drop in dissolved oxygen concentration to as low as 0.06 percent and a change from an aerobic to a virtually anaerobic state. By stopping the cell cycle, turbidity in the culture also stops increasing. The development of Metronidazole resistance in cells is a hallmark of anaerobiosis. When a granuloma has been steady for a significant amount of time, we consider it to be mature.

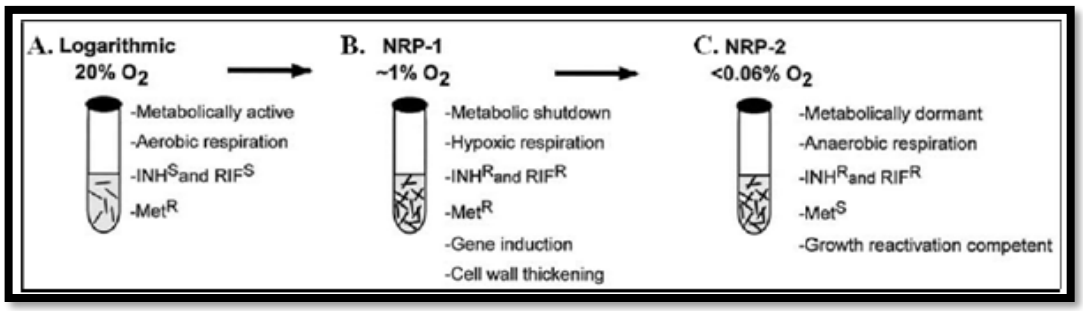

Figure 2: Hypoxia-induced Non-Replicating Persistent State Wayne Model Representation

There are three stages in total to the model. After the first stages of culturing cells, the oxygen content in the medium should have been rather high (logarithmic phase). Cultures susceptible to rifampicin (RIF) or metronizadole (INH), a drug used to treat anaerobiosis (Met). The B - NRP-1 state is defined by oxygen deprivation up to 1%, and it is characterised by bacterial resistance to INH and RIF and cell wall thickening. C - NRP-2 was demonstrated to be anaerobic and sensitive

to Metronidazole in cultures, despite having an oxygen level of less than 0.06%. These cultures in the NRP state were reactivatable under oxygen-poor conditions.

Other features of M. tuberculosis persistence, such as the stimulation of acr production inside macrophages (a protein similar to M. tuberculosis' crystalline protein), cannot be replicated by this approach. Because the bacilli are protected from oxygen deprivation and other environmental stresses inside the granuloma, acr expression has been demonstrated to be correlated with survival under these conditions by the research team of Cunningham and Spreadburg (1998).

To survive in an oxygen-free environment, tubercle bacilli, according to the Wayne model of latent infection, may switch to the glyoxylate pathway for NAD production. Drugs targeting different stages of the tuberculosis bacteria in the granuloma tissue have been shown to be effective in this animal.
Additionally, the Wayne model was used to construct an RGM model organism for M. tuberculosis chronic infection.

1.2. Nutrition Starvation Model

In this scenario, bacilli are believed to exist in an environment where they have limited access to vital growth nutrients and cofactors. This model confirms many significant results, including the alteration in colony form and the reduction of acid resistance. After growing in a nutrient-rich medium (PBS) for a while, bacteria are then moved to a nutrient-limiting medium (DMEM) and incubated there (Figure 2.10). Some of the bacilli's distinctive characteristics were as follows:

i) viability over 6 weeks.
ii) decreased rate of respiration.
iii) increased resistance to anti-tubercular drugs.

Colony shape and acid fastness were also affected in this bacillus strain; however, after the bacteria were returned to their original, nutrient-rich environment, the abnormalities were restored. Following a microarray analysis of nutrient-deprived cells, it was shown that expression levels of genes involved in the biosynthesis of all of the required substances were drastically reduced. This model concludes that a shift toward the production of secondary metabolites is necessary for host cell survival.

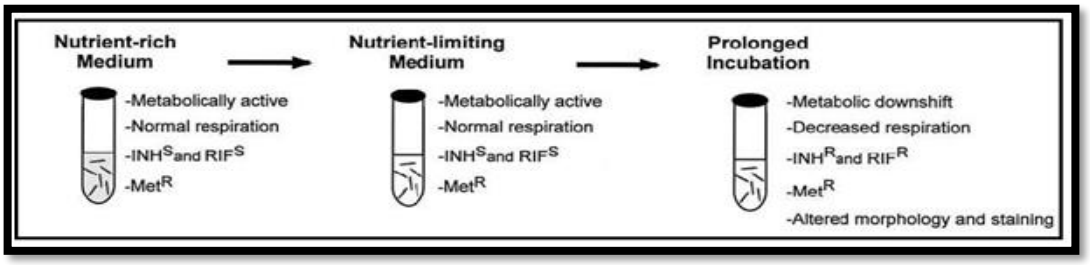

Figure 3: Representation of Nutrient Starvation Model.

After being cultured in a nutrient-rich medium for a while, the cells were put into a protracted nutrient-limiting incubation, where their metabolic rate dropped. Alterations in staining properties and colony form, as well as resistance to INH and RIF, were also produced in the bacteria.

1.3. *In vitro* Multiple-Stress Dormancy Model

During persistence, M. tuberculosis is exposed to a variety of stresses inside the host cell, which causes it to adopt a latent and drug-resistant phenotype. There are already available in vitro models that use a single stressor to mimic in vivo chronic situations. Multiple stressors, as opposed to a single stress situation, are experienced by the bacilli in the granuloma (as in the previous two models). Low oxygen levels, little CO_2 levels, low food input, and an acidic pH were shown to be the most effective conditions for culture growth. (5.0). Besides being unable to reproduce, the bacilli also changed in their acid resistance and phenotypic resistance to drugs. The genes responsible for making storage lipids were also identified as a potential target in the battle against latent M. tuberculosis infection.

1.4. *In vivo* Models

•Cornell Mouse Model

Cornell University's Mc Cune et al. developed the first animal model for latent TB in 1905. Mice were injected intravenously with virulent tuberculous bacilli and subsequently treated with antitubercular drugs (isoniazid and pyrazinamide) for 12 weeks to reduce bacterial populations (Figure 4). Following extensive treatment with antibiotics, bacteria were no longer present in infected tissues, and cell homogenates injected into animals were asymptomatic. Four weeks after finishing antibiotic treatment, the infection had persisted and reactivated.

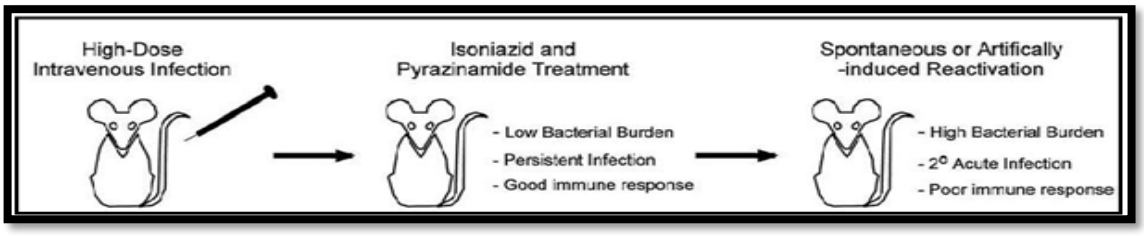

Figure 4: Cornell Mouse Model Representation

After receiving M. tuberculosis, mice were administered INH and pyrazinamide to reduce the bacterial load. The bacilli may remain dormant in the treated mice for an indefinite period of time before becoming active again.

It was shown that with this method, bacilli may be kept at undetectable quantities in host tissues, mimicking the physiological condition of human individuals. These models produced reactivation rates that were higher than those seen in humans.

• Low Dose Murine Model

The low-dose mouse model was created by inducing 57B/BALBc mice with M. tuberculosis (Figure 5). Bacillary proliferation was greatly reduced in the mice that were exposed to them, and the mice acquired a strong immune response to the bacilli. This is due to the fact that the model may accurately reflect human experiences, such as the fact that an adaptive immune response causes a growth plateau, and that bacterial growth is significantly slowed during an infection.

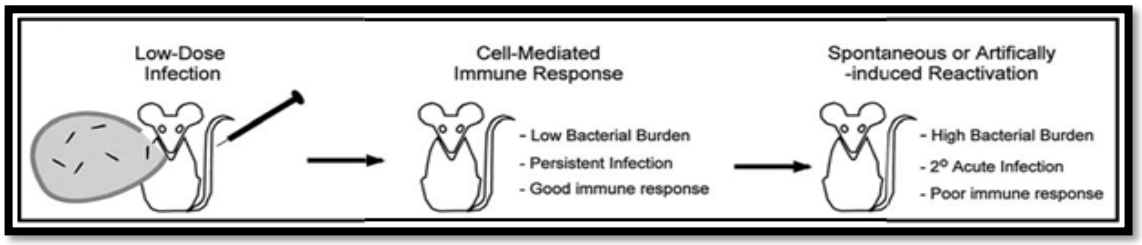

Figure 5: The Low-Dose Murine Model

The mice received a sublethal inoculum by injection or airborne spray. Adapted on Zahrt et alstudy .'s on mice with M. infectious TB, this model shows that mice develop a chronic form of the disease due to a robust immune response induced by cells after infection.
Reinfection rates in the model are similar to those seen in people, demonstrating the microorganisms' ability to survive.

• Mathematical Models

There are a number of mathematical models that attempt to portray the interactions between M. tuberculosis and its host during the course of TB infection. Researchers may collect data, put theories to the test, and extrapolate from experimental findings with the use of mathematical models. It's simple to grasp how a modification to either the bacterium or the host might alter the anticipated outcomes. These models may be used to make sense of the large amounts of unstructured data associated with the complicated human biological system.
There is still a need for experimental confirmation of many mathematical model predictions pertaining to tuberculosis (TB). Reactivation was predicted to be more frequent in the absence of IL-10 in mathematical models that mimicked IL-10 deletion, but this trait was not confirmed experimentally.
Researchers will continue to utilise mathematical models to deepen our knowledge of the transmission of infectious diseases.
As was said before, researchers are always finding new models for M. tuberculosis chronic infection. The stress response of tubercle bacilli was investigated by employing a nutrition restriction paradigm first proposed by Loebel. Since then, a plethora of other theories of persistence have been developed. One of the most significant models for hypoxia production is the in vitro human granuloma model, and another is the use of nitric oxide [NO] as an inhibitor. Dormancy model evolution is shown diagrammatically in Figure 6. Because of its ease of use for preliminary studies of persistence and reactivation and the speed with which it may be developed, the in vitro Wayne model remains the gold standard.

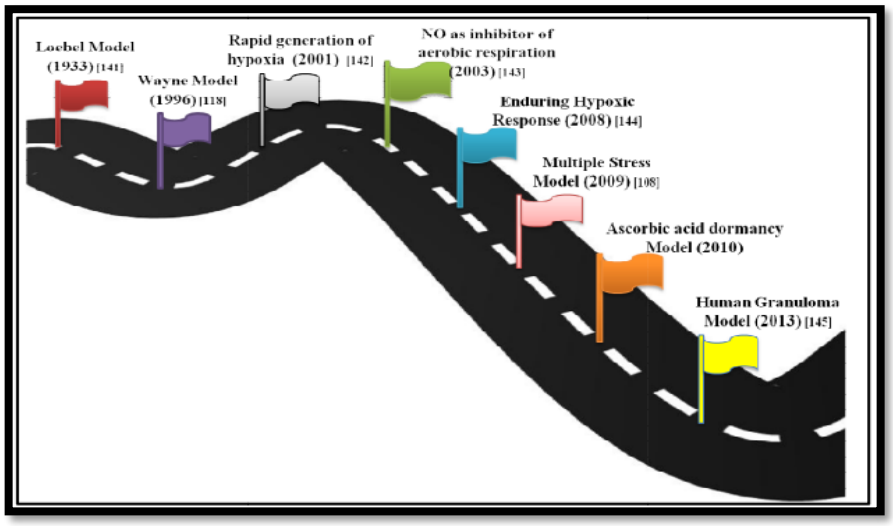

Figure 6: M. tuberculosis Evolution Dormancy Models

The evolutionary timeline, containing proposed models for M. tuberculosis dormancy persistence and the years in which they were proposed (Time not drawn to scale).

MATERIAL AND METHODS

Pathology

Lung tissues were preserved in 10% neutral buffered formalin for 48-72 hours before being paraffin embedded. Five micrometre thick tissue slices were stained with hematoxylin and eosin (H&E).

MIC DETERMINATION OF TOXIC METABOLITE ANALOGS

Mtb H37Rv (lysE, lysEcomp, and lysG) cells were grown to log phase in minimally supplemented media. Each version of the toxin was diluted twice in a sterile 96-well plate. Each drug was diluted in triplicate to final quantities of 0.2 mL and added to wells with an OD600 of 0.001. After incubating the plates at 37 °C for seven days, the optical density was measured using an Epoch plate reader (Biotek, Vermont, USA). The growth percentage was calculated based on the density of the wells that received no treatment. 50 g/ml of arginine was added to each well for the arginine rescue studies.

ISOLATION OF RELMTB AND RELMTBH80A

A fine balance between RelMtb's (p)ppGpp production and hydrolysis activities is necessary for normal TB homeostasis. Certain point mutations in RelMtb remove its ability to hydrolyze (p)ppGpp, but have no effect on the enzyme's ability to synthesise the molecule. We hypothesise that a RelMtb mutant in M. tuberculosis that lacks the ability to hydrolyze (p)ppGpp would exhibit phenotypic similarities to induction of the severe response.

Using plasmids, we cloned the relMtb gene from M. tuberculosis clinical strain CSU11/22 into pET15b and transformed it into E. coli. We also transformed pET22b, which contained the same relMtb gene but with a hydrolysis-ablating point mutation at amino acid 80 (relMtbH80A). Liquid cultures of Escherichia coli with the pET15b/RelMtb plasmid were turbid after four hours, but not after three days, whereas those with the pET22b/RelMtbH80A plasmid did not. The presence of the plasmids pET15b/RelMtbH80A and pET22b/RelMtbH80A was confirmed by performing a diagnostic digest on them using the enzymes and agarose gel electrophoresis. The existence of the intended plasmid and gene, pET15b/RelMtb, was confirmed by the appearance of the predicted DNA bands at 2214 and 5406 bp (Figure 7). When pET22b/RelMtbH80A was digested and the nucleic acids were measured using Nanodrop, no DNA bands were seen. Instead, a larger volume of pET22b/RelMtbH80A culture might be grown to achieve the same result. Plasmids pET15b/RelMtb and pET22b/RelMtbH80A were used to generate adequate samples for sequencing. Matching the resultant reads to the genetic sequence obtained from Tuberculist confirmed the existence of relMtb in the pET15b/RelMtb plasmid. When the genetic sequence of relMtb from Tuberculist was compared to the data obtained from pET22b/RelMtbH80A, however, no significant similarities were discovered. After isolating a copy of the pET22b/RelMtbH80A plasmid, we used the thermal shock method to transform a new strain of DH5 E. coli with it, therefore establishing the plasmid's presence. Despite the fact that a pUC19 control was successfully transformed, no detectable transformants were found on plates containing LB and ampicillin. In light of the unsatisfactory results from the diagnostic digest, Sanger sequencing, and transformation, it was decided to discontinue further work with this material in favour of synthesising a fresh relMtb from M. tuberculosis genomic DNA.

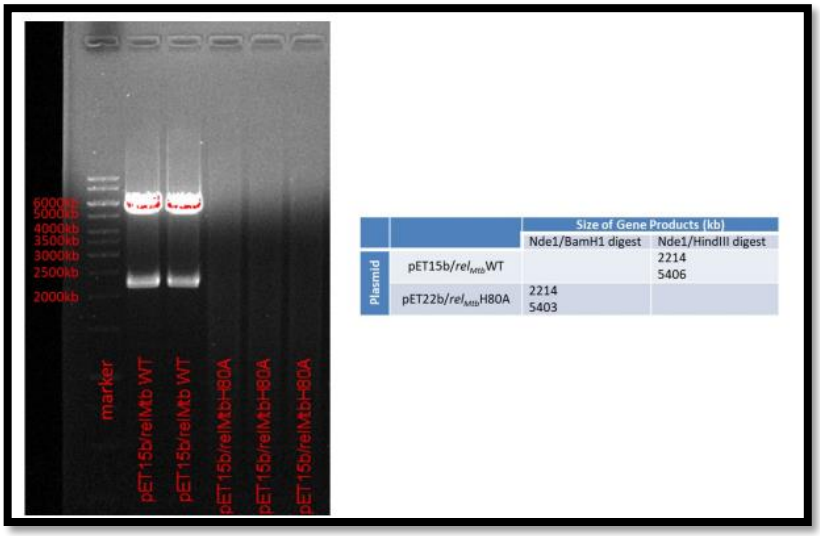

		Size of Gene Products (kb)	
		Nde1/BamH1 digest	Nde1/HindIII digest
Plasmid	pET15b/rel_{Mtb}WT		2214 5406
	pET22b/rel_{Mtb}H80A	2214 5403	

Figure 7: pET15b/RelMtb and pET22b/RelMtbH80A diagnostic digests Wild-type RelMtb (pET15b/RelMtb WT, lanes 3 and 4) or hydrolysis-deficient RelMtb (pET15b/RelMtbH80A, lanes 5-7) from plasmids containing pET15b were used to make the diagnostic digests. Band sizes predicted from plasmid size and restriction enzymes used.

SYNTHESIS OF HYDROLYSIS-DEFICIENT RELMTBD81A

The relMtb gene in the pET15b/RelMtb plasmid was derived from a clinical M. tuberculosis strain. RelMtb was cloned into pET15b using the RE list 2 after PCR amplification from a well-characterized M. tuberculosis laboratory reference strain H37RvSA using primers, and validated by Sanger sequencing with primers and BLAST analysis against the TB relMtb genomic sequence. This was done to keep things in line with the vast majority of the TB literature and with the results of previously published investigations. Changing either codon 80 or 81 causes RelMtb hydrolysis activity to be lost. Whereas codon 80 requires two different nucleotide substitutions, codon 81 just needs one. Site-directed mutagenesis was used to induce a point mutation in which aspartic acid was substituted for alanine, rendering the protein hydrolysis-inactive. The plasmid, tagged pET15b/RelMtbD81A, was analysed by BLAST against the genetic sequence of Tuberculous relMtb (Figure 8) and Sanger sequenced to verify its accuracy.

Figure 8: Sanger sequencing was used to confirm the site-directed mutation of relMtbD81A
A BLAST search of the wild type relMtb gene sequence against the probable relMtbD81A Sanger sequencing data. Boxed in red is the aspartic acid to alanine 81 nucleotide point mutation that disables hydrolysis.

CONFIRMATION OF PUV15TETORM PLASMID BACKBONES AND GENE INSERTION

An insufficient protein hydrolase due to overexpression The severe response is thought to be triggered by RelMtbD81A, which leads to decreased bacterial reproduction regardless of the number of nutrients available to the organism, via the dysregulated building of (p)ppGpp. On the other hand, researchers considered the possibility that mortality may result

from constitutive overexpression of RelMtbD81A. Consequently, we used a tetracycline-inducible method to induce the conditional overexpression of RelMtbD81A. Proteins from the herpes simplex virus virion and a tetracycline repressor (tetR) were fused in order to create a tetracycline regulated transactivator (tTA), which binds to the tetracycline response element (tetO) (TRE). Binding to this TRE, which is found upstream of a minimal promoter, activates production of the target gene. Tetracycline is taken off the TRE by the tetoff process, in which tetracycline is linked to TTA and then released. The current study increases the possibility of a significant response induction at the start of growth since it takes more than two days for tetracycline administration in the Tetoff system to lower gene expression. The tetracycline system, on the other hand, has a tTA that only binds to the TRE in the presence of tetracycline. By using this method, the bacterial cells may reach log phase before the expression of RelMtbD81A is triggered.

It was also important to consider the genomic stability of mycobacteria. L5 mycobacteriophage must be present for the attP attachment site and integrase to be integrated into the genomes of M. smegmatis, BCG, and M. tb. The integrase-assisted site-specific recombination is made possible by the presence of a homologous core region between the attP site on the plasmid and the attB attachment point in the bacterial genome. There has been a successful insertion of the plasmid sequence containing the gene of interest into the bacterial genome at the attB site. Including the gene of interest in the mycobacterial genome makes antibiotic selection unnecessary. Further, any in vitro phenotypes observed in animal models may be examined in animal models thanks to the use of the well-tolerated tetracycline analogue doxycycline to induce expression of the target gene.

Dr. YuMin Chuang, who has since left the lab, modified a plasmid donated to the team by Sabine Ehrt (Addgene plasmid #17975) to include an attP attachment site and an integrase that targets mycobacteria (pUV15tetORm). The plasmid's nucleotide sequence backbone was pUV15tetORm F. (Figure 9). Previous studies have revealed that M. tuberculosis harbouring the pUV15ttORm F plasmid backbone has a similar altered phenotype to wild type M. tuberculosis when tested with an empty vector control and a test plasmid containing the gene of interest. To determine if the unusual behaviour was caused by the gene of interest or the plasmid backbone, we flipped the promoter and reversed the TRE in the plasmid. The previously reported phenotypic shift only occurred with the pUV15tetORm R plasmid, which contains the gene of interest in reverse orientation, but not with the corresponding empty vector control. Consequently, the target gene, rather than the plasmid backbone, was credited with the observable phenotype.

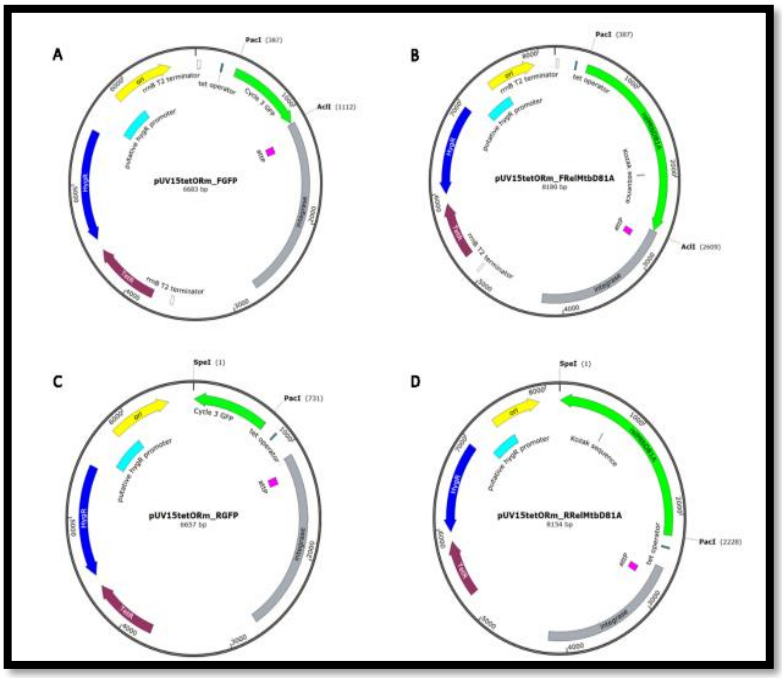

Figure 9: Peptide plasmid maps of pUV15tetORm F and pUV15tetORm R are available. A, B, C, and D show the plasmid maps for the various pUV15tetORm FRelMtbD81A mutants, as well as pUV15tetORm FGFP, pUV15tetORm RGFP, and pUV15tetORm FRelMtbD81A variants. Yellow represents the origin of replication; teal represents the tetracycline operator; green represents the gene of interest; pink represents the attP site; grey represents integrase; and the maroon coloration indicates the TetR repressor; and the red coloration indicates the hygromycin resistance cassette; (dark blue).

All plasmids submitted in for this study were verified using diagnostic digests to ensure their authenticity. The plasmids pUV15tetORm F and pUV15tetORm R were digested with the enzymes, and the results were seen on agarose gel electrophoresis. Two DNA bands of 1000bp and 5968bp or 387bp and 6552bp were seen after digesting pUV15tetORm F with AclI and PacI RE or SpeI and PacI RE, respectively (Figure 10), providing preliminary evidence for its

identification. When pUV15tetORm R was digested with either AclI and PacI RE or SpeI and PacI RE (Figure 10), the resulting DNA fragments were of the anticipated diameters (351 bp, 977 bp, and 5602 bp) and the expected lengths (1000 bp, and 5926 bp). In addition, Sanger sequencing using the provided primers and BLAST analysis against genetic sequences confirmed its accuracy. Both the pUV15tetORm F and pUV15tetORm R plasmid readings were determined to be included within the supplied plasmid sequences, with a similar percentage of coverage. It's more likely that the plasmids were missing parts of their projected sequence than that the readings didn't extend far enough to coincide with the next staggered scans. These missing chunks were either too small to detect or were situated in inconsequential parts of the plasmids that would not significantly alter the production of essential components. As a result, we concluded that the plasmids we had been using were the pUV15f and pUV15r variants of the pUV15tetORm. Instead of using an empty vector as a control, gfp was chosen since it provides a simple visual assay for confirming expression in vitro and in vivo. The Teton system has already used this gene for quality assurance purposes. Using primers designed for either pUV15tetORm F or pUV15tetORm R, we were able to clone gfp and relMtbD81A into the appropriate pUV15tetORm and pET15b/RelMtbD81A plasmid backbones. After performing a modified colony PCR using the aforementioned primers, we were able to confirm the existence of the gfp and relMtb genes by seeing DNA bands with sizes ranging from 500 to 750 kilobases. Sequencing using the primers and then performing a BLAST analysis against the genetic sequence of pUV15tetORm (Addgene plasmid #17975), a gift from Sabine Ehrt (Addgene plasmid #17975), and Tuberculist relMtb further confirmed the successful insertion of the gene. Following the discovery of gene insertions in each plasmid, the plasmids were given the names pUV15tetORm FGFP, pUV15tetORm RGFP, and pUV15tetORm FRelMtbD81A.

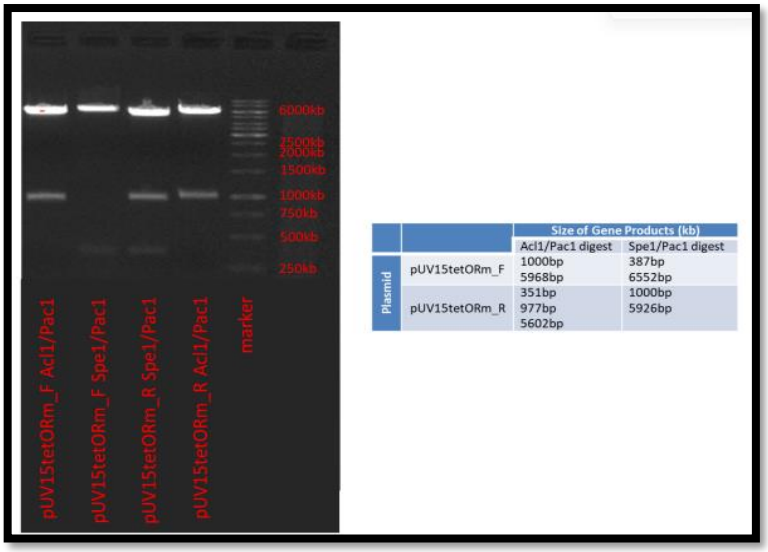

Figure 10: Digest of the F and R plasmids of pUV15tetORm There are two plasmid backbones, one for pUV15tetORm F (lanes 1 and 2) and the other for pUV15tetORm R (lanes 3 and 4). Predicted band diameters for various plasmid sizes and restriction enzymes.

ELECTROPORATION OF PLASMIDS INTO MYCOBACTERIUM SMEGMATIS

Mycobacterium smegmatis (M. smeg) is a fast-growing, nonpathogenic Mycobacteria strain that is often used as a stand-in for Mycobacterium TB (M. tuberculosis). The ability to hydrolyze (p)ppGpp and the ability to synthesise (p)ppGpp are both crucial for survival in high-stress environments. Because of these similarities, M. tuberculosis and M. smegmatis phenotypes are sometimes mistaken for those of one other. Experiments on M. smegmatis were initiated to confirm the concept and further the study of M. tb. There are three main types of fluorescent proteins that are often employed in the human body, and they are called FGFPI (FGFP), RGFPI (RGBFP), and FRELD81A (FRELD81A). M. smegmatis plasmids were electroporated into the host cell and then plated on 7H10 plates with 50 g/mL hygromycin. Single colony isolates were obtained after 4 days of incubation at 37°C; these colonies were PCR-amplified (Figure 11) and sequenced by Sanger using the appropriate primers to verify gene integration. There were three different strains of M. smegmatis developed: M. smegmatis FGFP, M. smegmatis RGFP, and M. smegmatis FRelMtbD81A.

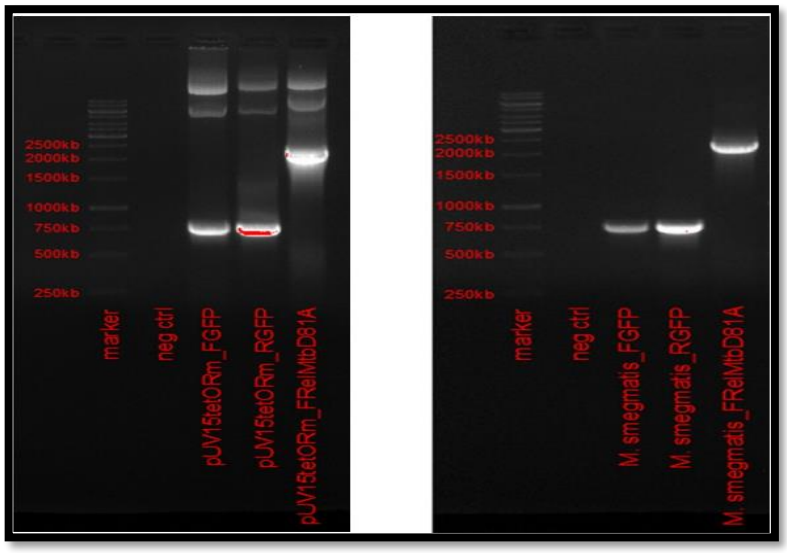

Figure 11: Confirmation of gfp and relMtbD81A insertion into plasmid backbones by PCR Agarose gel electrophoresis of PCR products from pUV15tetORm FGFP (gfp, lane 3), gfp, lane 4 and rel, lane 5 and confirmation of the gene insertion of interest by visualisation of the appropriate size DNA band (pUV15tetORm FRelMtbD81A).

qPCR

For the purpose of verifying the induction of gene expression of the target genes, qPCR was performed to measure gene expression at many time points over the course of three days. Within 48 hours of being exposed to the anhydrotetracycline inducer, M. smegmatis FRelMtbD81A relMtb expression had increased by about tenfold (Figure 12A). As a result, the number of remaining negative controls was either minimal or ambiguous.

Western Blot

We validated the concept by measuring protein expression over a span of three days using western blot analysis. Due to the presence of RelMsm in the strains utilised in this study, it was crucial to verify the specificity of the RelMtb antibody. As a result, a protein band of about 75 kDa was observed after 24 hours, 48 hours, and 72 hours when RelMtb antibody was probed into M. smegmatis FGFP and M. smegmatis FRelMtbD81A samples. M. smegmatis FRelMtbD81A samples showed a second protein band with the anticipated 82kd weight, restoring faith in the antibody's capacity to distinguish RelMtb from FGFP (Figure 12B). Further testing with the RelMtb antibody showed that RelMtb expression in M. smegmatis FRelMtbD81A increased continuously for up to 72 hours after the inducer was added (Figure 12C). The samples taken before 12 hours did not contain enough detectable protein to load a sufficient quantity of material onto a gel.

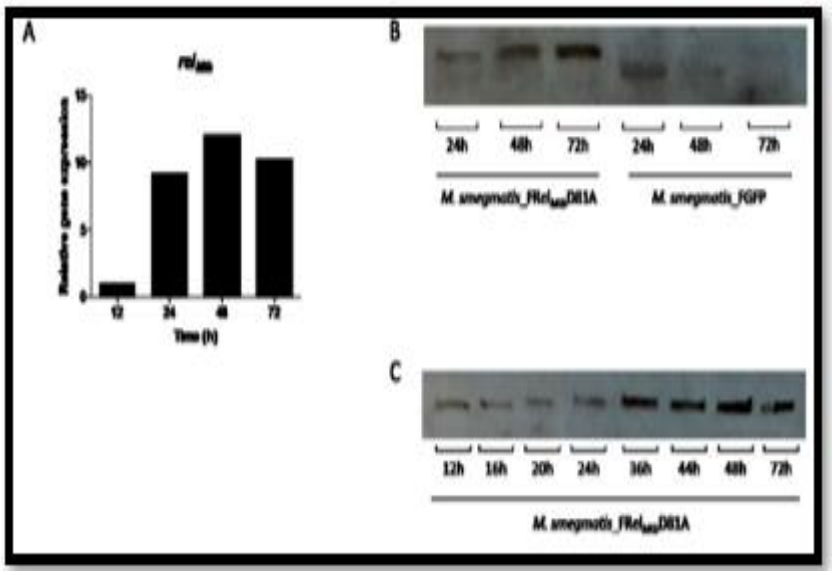

Figure 12: Gene and protein expression induction by anhydrotetracycline RT-PCR (A) and immunoblot (B) were used to monitor the temporal course of inducible expression (B, C) Anhydrotetracycline stimulation of relMtb gene expression at selected time points across a 72-hour time frame. Tests with RelMtb antibody against M. smegmatis FRelMtbD81A (Lane 3), as well as M. smegmatis FGFP (Lane 4-6) protein samples were used to confirm antibody

specificity for RelMtb throughout a 72-hour period. (C) A 72-hour time course of RelMtb protein expression after anhydrotetracycline stimulation.

GROWTH KINETICS

The goal of this study is to determine whether there are any differences in the rates of growth between M. smegmatis FGFP and M. smegmatis FRelMtbD81A. During the aforementioned window of time, we constructed a growth curve using the OD readings that were collected (Figure 13). None of the expected differences in growth kinetics between the two strains were seen in this growth curve.

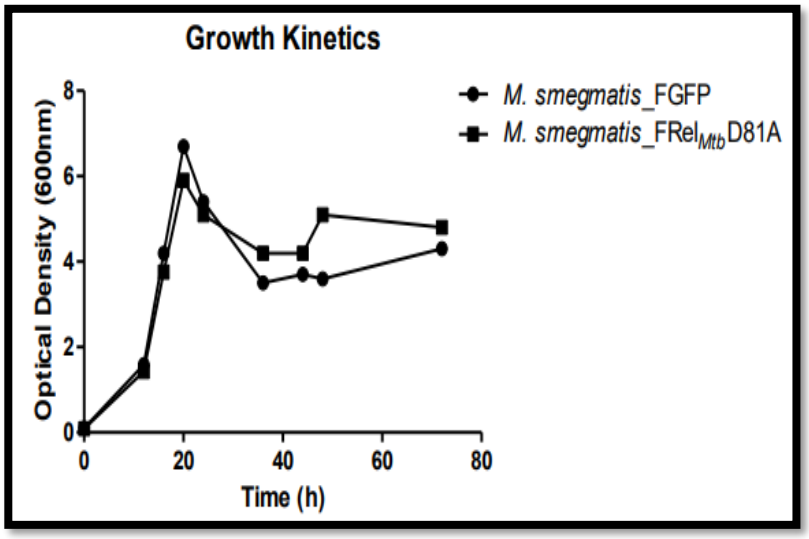

Figure 13: Kinetics of development Anhydrotetracycline stimulation of M. smegmatis FGFP and M. smegmatis FRelMtbD81A growth kinetics during a 72-hour period.

DISCUSSION

Persistent M. tuberculosis uses the stringent response pathway to slow its reproduction and metabolism, making it easier for antibiotics to kill it without causing it to evolve resistance. The effector molecule of this route is (p)ppGpp, and it is controlled in the bacterial cell by the bifunctional enzyme RelMtb. Achieving proficiency with the RelMtb function has the potential to Developmental Rates of Growth To sum up: 0 through 80 Optical density (h) of light for M. smegmatis infections (600nm) Plot No. 14 Speed and direction of change Growth kinetics of both M. smegmatis FGFP and M. smegmatis FRelMtbD81A after induction with anhydrotetracycline allow for fine-tuning of the stringent response. To influence whether M. tuberculosis enters a latent state or not has the potential to drive the bacterium into a more uniform population of replicating germs. Current first-line antibiotics, such as isoniazid, target reproducing bacteria, and they may be more effective against a homogenous population of bacteria than against a diverse population of bacteria for which they were not optimised.

An abundance of studies have examined how Rel affects bacterial development and adaptation. For more insight into the mechanism of this enzyme and its use in producing beneficial phenotypic changes, it may be useful to generate a knock-in strain that can trigger the stringent response and increase (p)ppGpp levels even in the presence of adequate feeding. Overexpression was achieved by introducing a point mutation into RelMtb at a known position that affects (p)ppGpp hydrolysis function and placing the gene under inducible promoter control. This allows the alarmone to build and the stringent response to be triggered by temporally regulating RelMtbD81A expression while maintaining (p)ppGpp synthesis function. Insertion of a forward-facing relMtbD81A gene and a GFP control gene into two different M. smegmatis genomes confirmed the inducible synthesis of RelMtb at the genetic and protein levels. We can now conduct practical tests with this strain.

A growth curve revealed that the kinetics of growth for the M. smegmatis FRelMtbD81A strain were identical to those for the control strain. This result was unexpected since it was hypothesised that when (p)ppGpp levels rose and the severe reaction was induced, the strain would reach a stationary phase earlier than the control strain. Optical density tests may be misleading because of variations in light refraction caused by stress-induced abnormalities in the bacterial cell wall, which may not necessarily reflect changes in viability. It has also been shown that the pUV15tetORm F backbone utilised to create the forward orientation M. smegmatis FGFP strain has an unfavourable in vivo phenotype. The in vivo findings favouring the forward orientation backbone provide a possible explanation for the lack of a phenotype in vitro. The pUV15tetORm F plasmid insertion is necessary to rule out the possibility that the M. smegmatis FRelMtbD81A or M. smegmatis FGFP strain has an identical phenotype to the original strain. The RelMsm deletion strain of M. smegmatis was found to be viable, however it performed worse in a competition assay when compared to the wild type strain. CFU

estimates were reported with greater precision by both groups. To solve the problems of ambiguous viability and the consequences of cell wall deformation inherent in the use of the optical density approach, a growth curve based on more accurate CFU counts is required for any future functional assessment of forward orientation strains of M. smegmatis. Possible explanations for the lack of a growth rate differential include the presence of native RelMsm. There is no reason to believe that RelMsm is prejudiced towards (p)ppGpp produced by RelMtbD81A. There may be no net increase in the amount of (p)ppGpp synthesised even if RelMtbD81A is responsible for this since the product may be hydrolyzed at the same rate at which it is generated.

In addition to verifying inducible production of RelMtb in the reverse orientation strain, further functional characterization of both the forward and reverse orientation RelMtbD81Astrains is required. To confirm that overexpressing RelMtb is sufficient to induce the stringent reaction and to gain insight into the effects of removing RelMtb's hydrolysis function, (p)ppGpp levels could be measured using high-performance liquid chromatography (HPLC), radioactive nucleotides, and thin-layer chromatography (TLC). Increases in poly(P) levels are a straightforward, if indirect, indicator of synthesis of (p)ppGpp. The higher presence of (p)ppGpp and the activation of the stringent response are hypothesised to cause the RelMtbD81A strain to develop more slowly and enter stationary phase earlier than the GFP control counterpart. Whether or whether bacteria will survive a too severe response is called into question when (p)ppGpp is overexpressed. If you suspect that your bacteria have been exposed to toxic levels of (p)ppGpp, a bacterial viability test can tell you if they have gone dormant or have died. An further aspect of a replication clock experiment that might provide light on bacterial growth rates is measuring the plasmid's persistence after twenty-one days. Plasmids are lost in the absence of antibiotics, and the rate of bacterial growth may be measured by plating bacteria on agar plates with and without antibiotics. By analysing this data, we can determine the reproduction rate of the bacterium under study. Because of higher (p)ppGpp, activation of the stringent response, and inhibition of replication, RelMtbD81A strains are predicted to retain more plasmid than control strains. This is because increased plasmid retention indicates a lower replication rate. The buildup of (p)ppGpp is correlated with antibiotic efficacy and so should be studied. When bacteria are subjected to increasing concentrations of antibiotic in a minimum bactericidal concentration (MBC) experiment, this concentration of antibiotic is thought to be the MBC. Notable, too, is the efficacy of isoniazid as a first-line therapy for eradicating RelMtbD81A strains. The ability of the RelMtbD81A strain to increase (p)ppGpp levels and activate the stringent response in nutrient-rich conditions is a good indicator that this strain will be resistant to isoniazid. Therefore, in nutrient-rich situations, the MBC of isoniazid should be greater than that required for wild type M. smegmatis. The plasmid constructs developed here might possibly be utilised to improve our knowledge of M. tuberculosis's proliferation and drug resistance characteristics. These tests would benefit greatly by using M. tuberculosis relMtb since it would eliminate the possibility of confounding effects from endogenous expression of RelMtb.

To improve the therapeutic response of phenocopy relMtb strains, using RelMtb small molecule inhibitors may also be helpful. Positive phenotypes may be elicited by small molecules, which might pave the way for their further study and potential development as therapeutics. If we can shorten TB treatment regimens by targeting the nonreplicating population of RelMtb, a potential druggable target, we may be one step closer to effectively treating people and eliminating TB from the world.

CONCLUSION

Experimenters used 13 to look into metabolomics. We used electrospray ionisation method to distribute column eluents. The hydrophilic interaction liquid-chromatography (HILIC) technique was used in conjunction with a 1.7 m anionic Acquity column (2.1 x 100 mm) for the UPLC study. Significant levels were found in the ThrB strain, but not in Rv or ThrA. 63. m/z = 120.0655. Since the bacteria need a lot of threonine for growth, we think this mass is homoserine. The m/z 120.0655 would be absent in a strain that cannot produce homoserine or threonine.

The 750 litres of supernatant were separated from the residual solids after a short incubation period in the freezer. Total RNA was isolated from the cell lysate via Direct-zol RNA MiniPrep (Zymo Research) and on-column DNase I digestion. Each pair of labelled probes was resuspended in hybridization buffer (500 litres formamide (20 percent SSC), 245 litres clean water (10 percent SDS)) and then placed to the microarray slide at a temperature of 42 degrees Celsius. After three separate 5-minute SSC cleaning cycles, the slides were ready for use. Concentration of 0.1 percent SDS, followed by three applications of 0.01% SSC for five minutes each and three applications of 0.1 percent SSC for five minutes each. A Genepix 4000A and a TIGR Spotfinder were used to scan the arrays. Tigris Midas then got to work on the data. The microarrays were inspected for flaws and clear spatial biases using two-color tiff pictures as a check. The slides that did not pass the quality check were hybridised again. Expression ratios were computed after normalisation of duplicate positions within the slides (total intensity and LOWESS). TIGR MeV software was used to perform a t-test using data from four independent biological replicates, each of which included two dye substitutions. The study's findings were used to provide rankings to the applicants. Genes with expression ratios larger than 2 and fewer than 0.5 were chosen based on a P-value of less than 0.05.

Purification of RNA from cell lysate samples was accomplished by using Trizol®-chlorofom precipitation as per the manufacturer's instructions (Invitrogen). R's DESeq2 software was used for the differential expression analysis. When researching mice, we adhered to the NIH's recommendations for the humane treatment of laboratory animals, published

in 1990. Bacterial burdens in the lungs and spleens were measured by killing four mice per group on days 1, 7, 21, 63, 84, and 98 (C57BL/6) or 1, 14, 22, and 42 (C57BL/6) to provide an accurate picture (SCID). Every group used six SCID mice for their survival rates. In order to perform conditional knockdown tests, infected mice were given doxycycline-treated chow (TestDiet, Missouri, USA) for 0, 1, 3, and 6 weeks. We killed four mice in each group, homogenised their lungs and spleens, and plated the organ homogenates on 7H10 medium with the appropriate supplement. According to rules, they were all kept in a lab designated as having a "level 3" animal biosafety enclosure.

Log phase was reached by cultivating Mtb H37Rv in lysE, lysEcomp, and lysG in minimally supplemented media. Each potentially lethal analogue was serially diluted by a factor of two in 96-well plates kept in a sterile environment. Each medication was diluted to an OD600 of 0.001 in three separate wells containing 0.2 mL each. The optical density of the plates was measured using an Epoch reader after seven days incubation at 37 °C (Biotek, Vermont, USA). Increase percentage was estimated using density data from wells that were not subject to any kind of treatment. As part of the arginine rescue trials, 50 g/ml of arginine was injected into each well.

As there are just a few number of known anti-tuberculosis targets, progress in finding novel medicines has been slow. The aspartate route in Mtb persistence metabolism has been shown to be particularly susceptible. For this reason, threonine and homoserine auxotrophs perish rapidly from Mtb infection. Due to threonine depletion, aspartate kinase becomes uncontrolled, leading to a flux imbalance and the buildup of lysine and diaminopimelic acid (DAP). Mtb's adaptive response to metabolic stress is a relief valve-like mechanism that involves the export of lysine and the degradation of aminoadipate. We show that long-term infections may be cleared up by inhibiting enzymes in the aspartate route at their various branch points. Our findings demonstrate the importance of many metabolic regulatory mechanisms for the aspartate pathway in Mtb.

REFERENCES

1. Berney, M. & Berney-Meyer, L. Mycobacterium tuberculosis in the Face of Host-Imposed Nutrient Limitation. Microbiol Spectr. 5, TBTB2-0030-2016 (2017).
2. Berney, M. et al. Essential roles of methionine and S-adenosylmethionine in the autarkic lifestyle of Mycobacterium tuberculosis. Proc. Natl Acad. Sci. USA 112, 10008–10013 (2015).
3. Connolly, L. E., Edelstein, P. H. & Ramakrishnan, L. Why is long-term therapy required to cure tuberculosis? PLoS Med. 4, e120 (2007).
4. Dartois, V. The path of anti-tuberculosis drugs: from blood to lesions to mycobacterial cells. Nat. Rev. Microbiol 12, 159–167 (2014).
5. Das, Priyanka & Janahiraman, V (2019). Analytical Study on Heterocyclic Anticancer Compounds. Research Review International Journal of Multidisciplinary; 4(5):172-175.
6. Das, Priyanka & Janahiraman, V (2019). Study on New Chalcones and Nitrogen Containing Heterocyclics. International Journal of Scientific Research And Review; 8(5):1069-1080.
7. Das, Priyanka & Srivastav, Alok Kumar (2014). Phytochemical Extraction and Characterization of the Leaves of Andrographis paniculata for Its Anti-Bacterial, Anti-Oxidant, Anti-Pyretic and Anti-Diabetic Activity. International Journal of Innovative Research in Science Engineering and Technology; 3(8):15176-15184.
8. Das, Priyanka & Srivastav, Alok Kumar (2015). A Comparative Study on Nutritive Values of Several Vegetables from West Bengal, Eastern India. International Journal of Pharmaceutical Research and Bio-Science; 4(1):381-390.
9. Das, Priyanka & Srivastav, Alok Kumar (2015). In-vitro Micropropagation of The Miracle Plant Aloe vera - A Method of Rapid Production. International Journal of Pure and Applied Research in Engineering and Technology; 3(11):12-27.
10. Das, Priyanka & Srivastav, Alok Kumar (2015). Phytochemical Extraction And Characterization of the Leaves of Aloe vera barbadensis For Its Anti-Bacterial And Anti-Oxidant Activity. International Journal of Science and Research; 4(6):658-661.
11. Das, Priyanka & Srivastav, Alok Kumar (2015). To Study the Effect of Activated Charcoal, Ascorbic Acid and Light Duration on In-vitro Micropropagation of Aloe vera L. International Journal of Innovative Research in Science Engineering and Technology; 4(5):3131-3138.
12. Das, Priyanka & Srivastav, Alok Kumar (2021). A Study on Molecular Targeted Approaches To Cancer Therapy And The Role of Chalcones In Chemoprevention. European Journal of Molecular & Clinical Medicine; 8(3):3254-3267.
13. Ehrt, S., Schnappinger, D. & Rhee, K. Y. Metabolic principles of persistence and pathogenicity in Mycobacterium tuberculosis. Nat. Rev. Microbiol 16, 496–507 (2018).
14. Eoh, H. et al. Metabolic anticipation in Mycobacterium tuberculosis. Nat. Microbiol 2, 17084 (2017).
15. Keren, I., Minami, S., Rubin, E. & Lewis, K. Characterization and transcriptome analysis of Mycobacterium tuberculosis persisters. MBio 2, e00100–e00111 (2011).
16. Pavelka, M. S. Jr. & Jacobs, W. R. Jr. Biosynthesis of diaminopimelate, the precursor of lysine and a component of peptidoglycan, is an essential function of Mycobacterium smegmatis. J. Bacteriol. 178, 6496–6507 (1996).
17. Puckett, S. et al. Glyoxylate detoxification is an essential function of malate synthase required for carbon assimilation in Mycobacterium tuberculosis. Proc. Natl. Acad. Sci. USA 114, E2225–E2232 (2017).
18. Ruecker, N. et al. Fumarase deficiency causes protein and metabolite succination and intoxicates Mycobacterium tuberculosis. Cell Chem. Biol. 24, 306–315 (2017).
19. Ghodke, Babasaheb Shivanath, Das, Priyanka & Srivastav, Alok Kumar (2022). An Analytical Study to Understand the Mechanism Behind Derailing the Aspartate Pathway of Mycobacterium Tuberculosis to Eradicate Persistent Infection. International Journal For Innovative Research In Multidisciplinary Field; 8(7):78-90.
20. Ghodke, Babasaheb Shivanath, Yadav, Sakshi (2021). Disrupting Mycobacterium Tuberculosis Aspartate Pathway in Order To Eliminate a Chronic Infection. Webology; 18(2):2571-2588.
21. Srivastav, Alok Kumar & Das, Priyanka (2014). Phytochemical Extraction and Characterization of Roots of Withania somnifera for Its Anti-Bacterial, Anti-Oxidant, Anti-Inflammation and Analgesic Activity. International Journal of Innovative Research and Development; 3(7):22-33.
22. Srivastav, Alok Kumar & Das, Priyanka (2014). To Study the Formulation of Niosome of Ofloxacin and Its Evaluation for Efficacy of Anti-Microbial Activity. International Journal of Innovative Research in Science Engineering and Technology; 3(12):17958-17965.
23. Srivastav, Alok Kumar & Das, Priyanka (2015). A Comparative Study of the Effect of Ampicillin and Tetracyclin on Bacterial Culture by Measuring the Zone of Inhibition. International Journal of Pharmaceutical Research and Bio-Science; 4(1):277-285.

24. Srivastav, Alok Kumar & Das, Priyanka (2015). Phytochemical Extraction and Characterization of Acorus calamus, Moringa oliefera, Cucurbita maxima, Hibiscus rosa sinensis and Chrysanthemum leucanthemum For Their Anti-Bacterial and Anti-Oxidant Activity. International Journal of Pharmaceutical Research and Bio-Science; 4(3):356-377.
25. Srivastav, Alok Kumar & Das, Priyanka (2015). To Study the Production and Standardization of Veterinary Vaccines. International Journal of Science and Research; 4(6):2331-2337.
26. Srivastav, Alok Kumar & Janahiraman, V (2019). Microbial Synthesis of Hyaluronan and Its Biomedical Applications. International Journal of Scientific Research And Review; 8(5):852-863.
27. Srivastav, Alok Kumar & Janahiraman, V (2019). Study on Microbial Production of Hyaluronic Acid. Research Review International Journal of Multidisciplinary; 4(5):231-233.
28. Trujillo, C. et al. Triosephosphate isomerase is dispensable in vitro yet essential for Mycobacterium tuberculosis to establish infection. MBio 5, e00085 (2014).
29. Viola, R. E. The central enzymes of the aspartate family of amino acid biosynthesis. Acc. Chem. Res. 34, 339–349 (2001).
30. Warner, D. F. Mycobacterium tuberculosis metabolism. Cold Spring Harb. Perspect. Med. 5, pii: a021121 (2014).
31. WHO. Global Tuberculosis Report 2017. (Geneva, Switzerland, 2017).
32. Zhang, Y. J. & Rubin, E. J. Feast or famine: the host-pathogen battle over amino acids. Cell. Microbiol. 15, 1079–1087 (2013).
33. Zhang, Y. J. et al. Tryptophan biosynthesis protects mycobacteria from CD4 T-cell-mediated killing. Cell 155, 1296–1308 (2013).